J. Fluid Mech. (1980), *vol.* 100, *part* 3, *pp.* 639–668
Printed in Great Britain

Measurements of interacting turbulent shear layers in the near wake of a flat plate

By J. ANDREOPOULOS† and P. BRADSHAW
Department of Aeronautics, Imperial College, London

(Received 19 June 1979)

Measurements of velocity fluctuations in the wake of a thin non-lifting aerofoil are presented: in one set of experiments the flow was symmetrical, while in the other the upper surface of the aerofoil was roughened to increase the surface shear stress. Measurements were confined to the near wake, where the disturbed region lies within the inner layers of the original boundary layers; thus the boundary-layer thickness is not a relevant length scale. The practical relevance of the experiment is to the prediction of flow over aerofoils, where only the initial region of the wake significantly affects the aerofoil pressure distribution. Temperature-conditioned sampling techniques were used, one boundary layer at a time being heated so that fluid from each boundary layer could be traced within the wake. In contrast to the behaviour of merging shear layers in ducts and jets, the wake interaction involves significant fine-scale mixing; the results reveal a three-layer structure, with a fine-scale inner wake of mixed fluid separating two layers in which structural changes are confined to the region of time sharing, or internal intermittency, between mixed and unmixed fluid. The implications of the results for calculation methods are discussed.

1. Introduction

This paper is one of a series on 'complex' turbulent flows (defined as shear layers with complicating influences like distortion by extra rates of strain or interaction with another turbulence field). General reviews of complex flows are given by Bradshaw (1975, 1976). The latest of the papers on extra rates of strain is that by Hoffmann & Bradshaw (1978). The present paper is a sequel to those by Dean & Bradshaw (1976) on interacting turbulent boundary layers in a duct and by Weir, Wood & Bradshaw (1980) on interacting turbulent mixing layers in a jet. The object of the present work is to study the way in which unidirectional turbulent shear layers such as the boundary layers on the upper and lower surfaces of an aerofoil interact after they meet, in this case at the trailing edge of the aerofoil. In the present state of non-universality of calculation methods for turbulent flow it seems likely that adequate predictions for these rather complicated, asymmetrically interacting flows will be obtained only by treating the interactions explicitly, as in the 'superposition' calculation methods published by Bradshaw, Dean & McEligot (1973), Morel & Torda (1973) and Huffman & Ng (1978). These calculation methods all involve the solution of equations for two components of shear stress, one for each layer, the interaction being represented by a 'time-sharing' process in which shear stress of either sign

† Present address: SFB 80, Universität Karlsruhe, Federal Republic of Germany.

0022-1120/80/4561-2220 $02.00

can occur at the same place but not at the same time, as eddies enter the interaction region from either side more or less alternately. Exact superposition is of course forbidden by the nonlinearity of the Navier–Stokes equations, but the use of superposition in the mathematical model is equivalent to the experimentally observed process: time sharing without noticeable change in the turbulent structure parameters of one shear layer after it merges with the other.

In the case of the duct, superposition (or time sharing) appears to be an extremely good approximation to the experimental results, and good agreement with experiment was obtained by a calculation method based on superposition and using turbulence structure parameters typical of isolated boundary layers, even for the case of fully developed flow. The implication is not only that the large eddies at the outer edges of each boundary layer time-shared without noticeable change in their turbulence structure, but also that the transfer of fluid from one set of large eddies to the other by fine-grained mixing had negligible local effect. The cumulative effect of fine-grained mixing must eventually be to mix all the fluid from both sides of the duct, although the large eddies from either side of the duct would continually re-form and thus be identifiable far downstream. In the case of the merging of two mixing layers to form a two-dimensional jet (Weir *et al.* 1980) significant changes in turbulence structure parameters were found. The reason seems to be that the typical turbulence intensities in mixing layers are higher than in boundary layers so that the interaction is more intense and nonlinear effects are more likely to occur. Fine-grained mixing, however, still seems to be relatively unimportant in this case.

The distinction between the duct and jet on the one hand, and the wake of a streamlined body on the other, is that in the former cases the merging occurs by meeting of the high-speed sides of the shear layers and the gradual disappearance of the potential-flow region between them. That is, the interaction occurs between two well-formed groups of large eddies of similar length scales on the two sides. (It should be noted that, although the above-mentioned experiments were performed on symmetrical flows, the general dynamics of the interaction will be the same in asymmetrical flows as long as the length scales on the two sides are of the same order of magnitude.) In the case of the wake, however, the interaction initially takes place, downstream of the trailing edge, between the inner layers of the low-speed sides of the two turbulent boundary layers, whose eddy size was previously confined to be proportional to the distance from the wall. That is, the interaction in the wake is essentially fine-grained mixing rather than the time sharing of large eddies. Outside the region of fine-grained mixing the changes in turbulence structure are expected to be relatively small. Once the region of fine-grained mixing (hereafter referred to as the 'inner wake') has spread beyond the inner layers of the original boundary layers, it may be expected that the large eddies in the outer parts of the two boundary layers will interact more strongly, until far downstream the classical fully developed wake is obtained. The present experiment covered only the initial region, in which the inner wake is confined to the inner layers of the original boundary layers, because the practical interest in the flow was in the prediction of the pressure distributions around aerofoils; in this case the displacement thickness of the wake more than a few boundary-layer thicknesses downstream of the trailing edge has very little effect on the flow around the aerofoil itself. From the fundamental point of view, of course, the restriction to short distances downstream and the absence of large-eddy interaction makes the results easier to

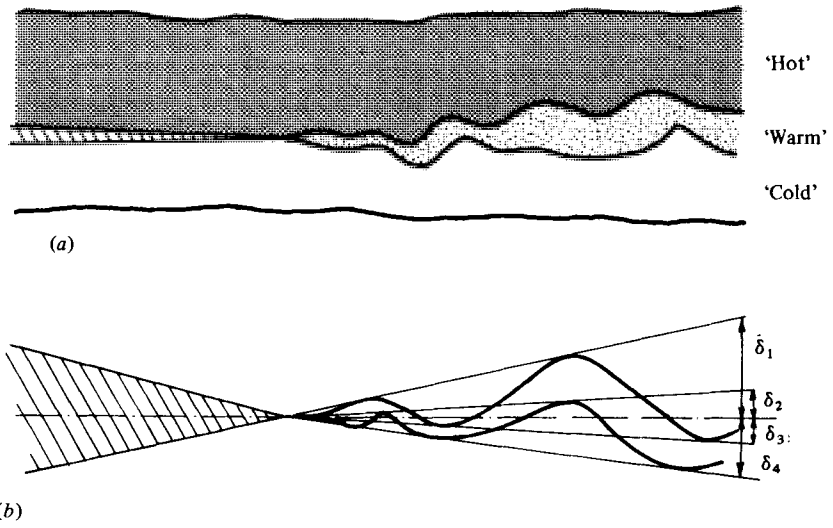

FIGURE 1. Near-wake configuration. (*a*) 'Hot', 'warm' (mixed) and 'cold' regions; upper boundary layer heated; (*b*) definitions of mixed-region thicknesses (instantaneous shape highly idealized, vertical scale magnified).

interpret. In particular, inner-layer scaling, based on the friction velocity at the trailing edge of the aerofoil, should be applicable to the inner wake. In contrast to the duct and jet experiments, we have studied both symmetrical and asymmetrical wakes: in the latter case, the ratio of the friction velocities on the upper and lower surfaces of the aerofoil is an additional parameter in the inner-layer scaling.

Since the effects of moderate pressure gradients on the structure of turbulent flow are indirect and fairly well understood, we decided for simplicity to consider only the wake of a thin flat plate, the asymmetrical case being set up by roughening one side of the plate so as to provide a boundary-layer of greater skin-friction coefficient and greater thickness on that side. The symmetrical configuration was similar to that used by Chevray & Kovasznay (1968), although the Reynolds number was roughly 10 times higher in the present case and the experimental techniques were more sophisticated. We are not aware of any work on simple asymmetrical near wakes – the work of Palmer & Keffer (1972) was done far downstream of a bluff body – and the rather large amount of data on near wakes of conventional aerofoils seems not to include any worthwhile turbulence measurements. As in the duct and jet experiments, and in the work of Fabris (1974) and LaRue & Libby (1978) on far wakes, temperature-conditioned sampling was used. The boundary layer on one side of the plate was heated slightly and a fast-response wire resistance thermometer located very close to the hot-wire probe was used to discriminate between 'hot' and 'cold' fluid, which could therefore be identified as coming from either the heated or the unheated side of the plate even after the shear layers had started to interact. It will be seen below that this technique can actually be used to distinguish hot, warm and cold fluid, where the 'warm' fluid is that resulting from fine-grained mixing in the inner wake. As can be seen from the sketch of figure 1, the instantaneous boundaries of the inner wake are sinuous – the probability of the fluid on the centre-line being either fully hot or fully cold is about 0·14 in the symmetrical case – and it is because the boundaries between

the three regions are fluctuating in this fashion that conditionally sampled averages are necessary to investigate the dynamics of the flow. It is not anticipated that calculation methods based on these experiments would use conditional averages explicitly but the intermittency of the hot, cold and warm processes would be implicit in the choice of turbulent structure parameters. The results show highly spectacular differences between the conditional averages for the different regions. For instance, near the edges of the inner wake the contribution of the unmixed fluid to the triple products is opposite in sign to the contribution of the finely mixed 'warm' fluid, which is indeed what one would expect if the two layers were genuinely different. The results leave no doubt that even this rather sophisticated use of conditional sampling reveals real differences in flow structure rather than generating insignificant statistics. These structural differences should be represented in calculation methods, at least those intended for general, asymmetric flows. Our own work on calculation methods for interacting shear layers is being reported separately.

Section 2 of this paper briefly describes the experimental techniques, which are an improvement on those used by Dean & Bradshaw and are discussed more fully in the paper by Weir *et al.* (1980). Section 3 presents a selection from the results; more detail is available in the thesis by Andreopoulos (1978). The results presented here are chosen to illustrate the discussion in § 4. A main conclusion is that the three-layer model shown in figure 1, in which the outer regions formed by the original boundary layers are virtually undisturbed except near their boundaries with the inner region of finely mixed fluid, provides a simple and effective method of describing and calculating the flow. In particular, it is found that the shear stress in the mixed fluid can be quite well described by an eddy viscosity. The eddy viscosity for the mixed fluid is positive and well behaved everywhere, even in the asymmetrical case (in which the overall eddy viscosity has a significant negative region between the point of zero shear stress and the point of zero velocity gradient).

2. Experimental arrangement

The experimental programme was carried out in the 91 × 91 cm (3 × 3 ft) closed-circuit low-speed wind tunnel of the Department of Aeronautics at a free-stream speed U_e of 33 m s^{-1}. The free-stream turbulence level in the wind tunnel is less than 0·05 % at this speed. The flat plate was 3·08 m long and spanned the wind tunnel at mid-height. The plate was made of plywood 28 mm thick, with a streamlined nose and a straight taper over the last 0·45 m giving a total included angle at the trailing edge of 3·5°. The tapered portion was made from 1 mm thick aluminium sheet with plywood ribs and a final extension made of 0·05 mm thick steel shims giving a trailing edge thickness of nominally 0·1 mm. The plate thickness and construction were chosen to minimize heat transfer from one side to the other. The 'hot' side of the flow was heated by nichrome wires a few millimetres from the surface near the leading edge of the plate. The boundary-layer thickness at the trailing edge was at least 50 mm so that the heated wakes of the wires were fully mixed into the turbulent flow. Since the boundary layer continues to entrain cold free-stream fluid, the temperature profile at the trailing edge is not uniform. However, the temperature in the inner layer, say $y/\delta < 0{\cdot}1$, was nearly constant and 1·5–2 °C above the ambient temperature. The root-mean-square temperature fluctuation in this region was roughly 0·15 °C,

rising to 0·4–0·5 °C in the outer part of the boundary layers. The temperature-conditioned sampling techniques used here do not rely on the 'hot' fluid being at uniform temperature but merely on negligible penetration of unheated free-stream fluid down through the heated boundary layer to the surface. This negligibility is guaranteed by the fact that the intermittency factor for velocity or temperature is unity for y/δ less than about 0·4. Dummy wires were installed near the leading edge on the unheated side of the plate in order to maintain symmetry of the velocity field.

For the asymmetrical case, the entire upper surface of the plate was covered with sandpaper with a maximum grain size of about 1·4 mm. The boundary layer at the trailing edge is discussed in detail by Andreopoulos & Bradshaw (1979). The shift in the logarithmic law compared to that on the smooth surface is about $-11u_\tau$. The use of roughness rather than pressure gradient to obtain an asymmetrical flow has the advantage that the shear stress gradient $\partial\tau/\partial y$ near the surface is small; that is, the flow in the inner wake is defined (according to inner-layer scaling arguments) by the friction velocities on the rough and smooth sides, $u_{\tau r}$ and $u_{\tau s}$ respectively, by the viscosity, and by the co-ordinates x and y measured from the trailing edge. In more complicated cases the shear stress gradient $\partial\tau/\partial y$ each side of the trailing edge would also affect the flow. We believe that we have chosen the simplest kind of asymmetrical wake that demonstrates the physical features of such asymmetry. The thickness of each boundary layer at the trailing edge in the symmetrical case was 53 mm ($\theta = 6{\cdot}35$ mm, $U_e\theta/\nu = 13600$, $c_f = 0{\cdot}0024$) while in the asymmetrical case the boundary layer on the upper roughened surface was 76 mm ($\theta = 10{\cdot}2$ mm, $c_f = 0{\cdot}0052$) and that on the lower surface 51·5 mm. In all cases the thickness is defined as the distance from the surface to the point at which the velocity reaches 0·995 of the free-stream value. Fuller details of mean flow parameters are given in table 1.

Turbulence measurements were made with DISA type 55D01 constant-temperature anemometers and DISA miniature cross-wire probes type 55A38 with 5 μm platinum wires. Temperature fluctuations were measured with 1 μm 'cold wires' mounted on probes clamped to the side of the cross-wire probe, the centre of the temperature sensor being within 1 mm, i.e. one wire length, of the centre of the cross-wire probe; the smallest thickness of inner wake for which results are presented is about 10 mm ($x = 25$ mm, see figure 6) so that even in this case spatial resolution should be acceptable.

The cold wire was operated by a constant-current circuit with a heating current of not more than 1·6 mA, the temperature sensitivity being at least two orders of magnitude greater than the velocity sensitivity in all cases. A more important source of contamination of the temperature signal was spurious temperature fluctuations in the nominally unheated boundary layer, caused partly by heat transfer through the plate and partly by the finite heat capacity of the plate itself in the presence of a gradually increasing tunnel temperature. However, the spurious temperature fluctuations did not interfere significantly with the discrimination process. The temperature-wire output was compensated by a conventional operational-amplifier network. The compensation was adjusted so as to obtain the sharpest possible rise and fall of the temperature signal at the leading and trailing edges of bursts of hot fluid, while avoiding an 'overshoot' of temperature below the free-stream value. This technique, of course, tends to suppress the effect of thermal conductivity in reducing

the temperature gradient at the edges of the hot and cold regions but this was felt to be a negligible effect in the present high-Reynolds-number experiment. Since the Prandtl number of the fluid is of order unity (0·72) the thicknesses of the conductive layer and of the corresponding viscous layer are about the same. Analog compensation of the cold-wire signal was necessary because of the need to adjust the compensation in real time, but linearization of the hot-wire signals and allowance for the contamination of the hot-wire signals by temperature fluctuations was carried out digitally. Signals from the cold-wire probe and from the two hot wires of a cross-wire probe were recorded on an Ampex FR1300 analog tape recorder at a tape speed of 60 in./s, giving an analog bandwidth of 20 kHz which corresponds to a wavelength of about 1·5 mm at a speed of 30 m s^{-1}. This is compatible with a wire length of 1 mm, which limits the spatial resolution. The signals were later replayed, at a tape speed of 15 in./s, into an analog-to-digital conversion system operating at 20000 samples per second total digitization rate, and recorded on a computer-compatible digital magnetic tape. The inputs to the analog-to-digital converter were filtered at the folding frequency, giving a real time analog response of 13 kHz. The conditional-sampling algorithm used is the same as that described by Weir *et al.* (1980) and more fully by Weir & Bradshaw (1974). Fluid is labelled 'hot' if its temperature exceeds the base level by more than a certain threshold value, usually 0·1 °C. However, data points are also labelled 'hot' if the time derivative of the temperature exceeds a certain small value. This helps to distinguish the beginning and end of hot periods as sharply as possible. The algorithm also deals with slow drift of the baseline 'cold' level, although this was a much less serious problem in the present experiment than in the jet experiment of Weir *et al.* (1980). No explicit 'hold' time is used; in critical cases the temperature history over the last few digitization points is inspected to see if a given hot–cold or cold–hot transition is real, but in all cases hot or cold bursts of one digitization interval, equivalent to 0·028, are permissible.

We have not investigated 'bursting frequencies' in the present experiment, believing that the only logical way to treat bursting frequencies is by way of a probability distribution of burst length (Murlis, Tsai & Bradshaw 1980); a single average bursting frequency is no more realistic than an 'average turbulent frequency'. All products of velocity fluctuations u and v and temperature fluctuation θ up to third order were evaluated by the analysis program, together with $\overline{u^4}, \overline{v^4}$ and the intermittency factor. 'Hot', 'cold' and conventional averages were available in each case. The results presented here measure all fluctuations with respect to the conventional-average velocity or temperature, since measuring with respect to zonal averages automatically rejects the fundamental contribution to the velocity excursion within the zone. The conditional-average products of velocity fluctuations are presented as *contributions* of the hot and cold zones to the conventional average: that is, the zone contributions sum to give the conventional average. This gives a better idea of the importance of each zone than the presentation of zonal averages as such. The hot-zone contribution (for example) is simply γ times the hot-zone *average*, so that the zonal averages can easily be recovered from the results if required.

The basic temperature-discrimination technique is, of course, a 'hot–cold' one, incapable of distinguishing fully-hot fluid from mixed fluid that is merely 'warm'. Figure 2 shows highly idealized temperature traces near the centre-line of the wake, in which the signal alternates between a low 'cold' level and a high and supposedly

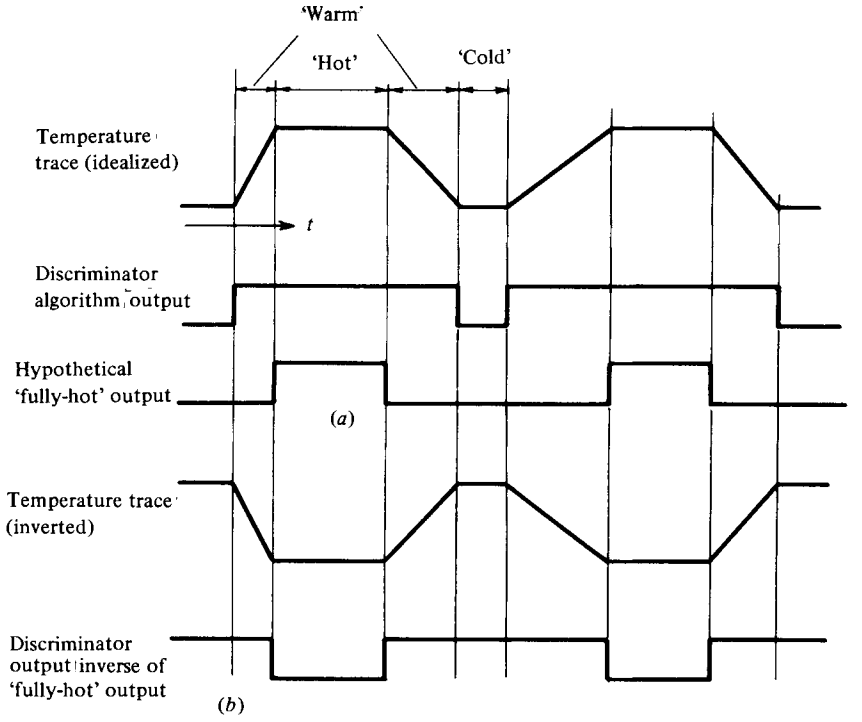

FIGURE 2. Deduction of 'warm' (mixed-region) averages from algorithm which distinguishes only 'cold' and 'warm *or* hot'. (*a*) Upper boundary layer heated, (*b*) supposed exact repeat with lower boundary layer heated.

uniform 'hot' level, via fairly slow transitions which are here referred to as 'warm'. The output of the hot–cold discrimination algorithm corresponding to the temperature trace in figure 2(*a*) is shown immediately below it. If the fully hot fluid were really at uniform temperature, it would be possible to distinguish it by using a threshold setting just *below* the fully hot level itself, obtaining the bottom trace in figure 2(*a*), but it was not possible to do this in the present case because the upper temperature level actually varied considerably. A simple alternative approach was adopted. Supposing for purposes of exposition that it was possible to reproduce the instantaneous fluctuations exactly in a second experiment, it would be possible to do one experiment with, say, the upper boundary layer heated, and a second experiment with the lower boundary layer heated. The second experiment would then give the temperature trace shown in figure 2(*b*), whose cold intervals correspond to the fully hot intervals in figure 2(*a*) and for which the intermittency algorithm gives the trace shown at the bottom of figure 2(*b*). Now the warm regions are simply given by the overlapping portions of the plateaux in the intermittency traces of figure 2(*a*) and of figure 2(*b*), and the warm-zone contributions to the averages can be obtained by subtracting the cold-zone contributions of figure 2(*b*) from the hot-zone contribution of figure 2(*a*) or vice versa.

It is not, of course, possible to reproduce an experimental instantaneously in practice but it is possible to repeat the experiment with the other boundary layer heated and obtain *averages* which obey the subtraction law just stated. In the case

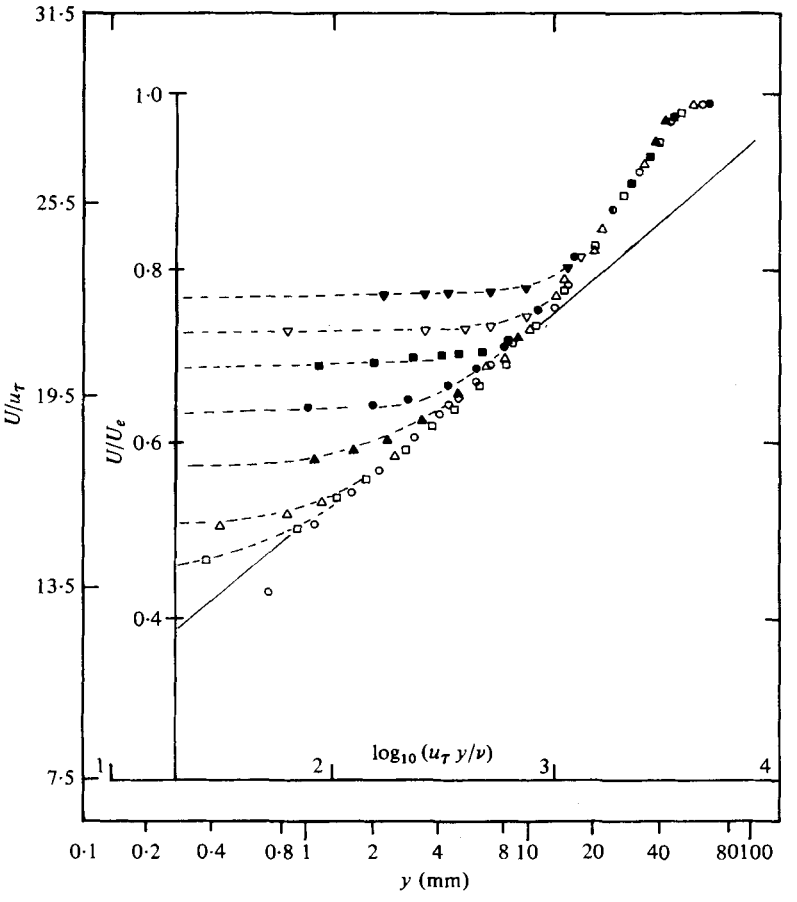

FIGURE 3. U-component mean-velocity profiles in symmetrical wake. Values of x (mm): ○, 0; □, 10; △, 20; ▲, 50; ●, 100; ■, 200; ▽, 300; ▼, 500.

of the symmetrical flow, it is not even necessary to repeat the experiment with the other surface heated, because the results of that experiment are trivially easy to deduce by symmetry. In the asymmetrical case it was, however, necessary to do one set of experiments with the upper boundary layer heated and one with the lower boundary layer heated. To avoid confusion the zonal averages presented below are simply labelled 'mixed' and 'unmixed' fluid, with the further distinction of whether the unmixed fluid in the asymmetrical case originated on the rough-wall side or on the smooth-wall side. The realism of the distinction between mixed and unmixed fluid, and the accuracy of the methods by which it is made, are demonstrated by the way in which the profile of the unmixed-fluid contribution to some turbulent average tends smoothly and monotonically to zero, even when the mixed-fluid contribution is large and of opposite sign. There was little indication in the present results of the negative loops found by Dean & Bradshaw in some of the zonal-contribution profiles in the duct flow. These negative loops arose partly because Dean & Bradshaw's algorithm lumped together the 'warm' and 'fully hot' fluid. In the case of the duct this was not too serious, but complete neglect of fine-grained mixing in the present experiment would have led to totally different results of no great practical value.

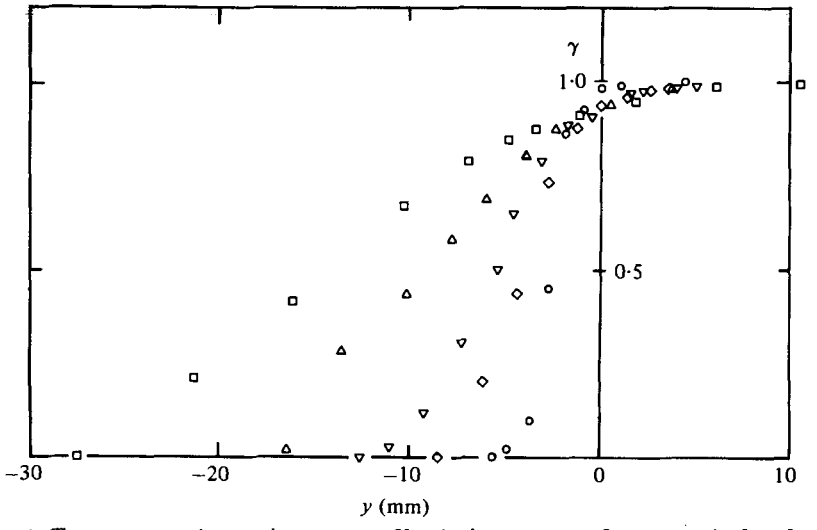

FIGURE 4. Temperature intermittency profiles in inner part of symmetrical wake (upper boundary layer heated). Values of x (mm): ○, 25; ◇, 50; ▽, 100; △, 200; □, 400.

3. Results

Figure 3 shows mean velocity profiles for the symmetrical wake plotted on semi-logarithmic axes, the centre-line $y = 0$ corresponding to $\ln y = -\infty$. It is seen that the edge of the disturbed region is quite distinct and that the outer part of the velocity profile is virtually unaltered. This is in fact the coincidental result of two small opposing effects, the slow growth of the boundary layer into the external stream and the small negative value of V induced in the outer layer by the acceleration near the surface. However, the turbulence measurements shown later indicate that the outer part of the layer is effectively unperturbed by the mixing in the inner wake, and outer-layer results will not be presented in detail except for the trailing-edge position. The ratio of the centre-line velocity to u_τ should be a universal function of $u_\tau x/\nu$ according to inner-layer scaling and a good fit to the present symmetrical results is

$$\frac{U_{\mathrm{CL}}}{u_\tau} = 4{\cdot}65 \log_{10}\left(\frac{u_\tau x}{\nu}\right) + 0{\cdot}7 \tag{1}$$

although an exactly logarithmic variation is not to be expected. Chevray & Kovasznay's data seem to follow a similar trend although with a slightly larger intercept and slope.

Figure 4 shows the temperature-intermittency factor at different positions downstream. According to the discussion in § 2, $(1-\gamma)$ is the probability that the fluid at a given position is 'cold', i.e. that it is unmixed lower-surface fluid in the present case where the upper boundary layer is heated. Thus, the probability of finding unmixed lower-surface fluid on the centre-line is about 0·07; the probability of finding unmixed upper-surface fluid on the centre-line must also be 0·07 and so the probability of finding finely mixed 'warm' fluid on the centre-line is 0·86. That is, the 'warm' region is sinuous, as shown in figure 1 which exaggerates the amplitude of the large-scale undulations but probably underestimates the small-scale irregularities of the instantaneous boundaries. We refer to the warm fluid as 'finely mixed' simply to emphasize

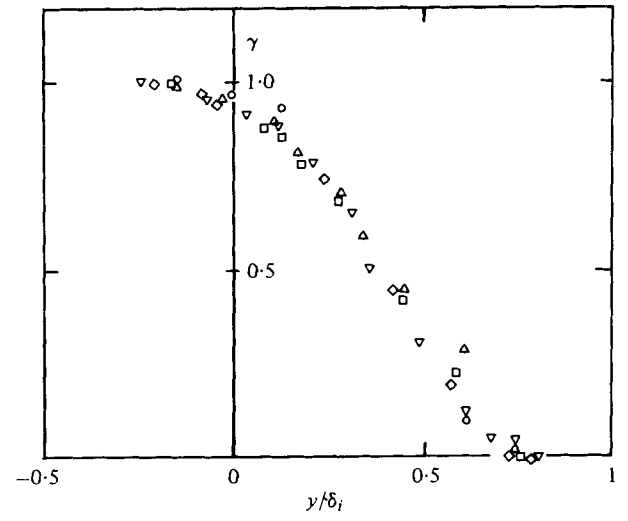

FIGURE 5. Temperature-intermittency profiles scaled by profile widths δ_i (see table 1). Symbols as in figure 4.

(*a*) Symmetrical case

x	$2\times\delta_{995}$ (mm)	δ^* (mm)	θ (mm)	H	θ/θ_0	δ_1	δ_3	$\delta_\gamma\equiv\delta_1+\delta_3$	δ_τ
0	107·1	16·2772	11·8127	1·37793	1·000	—	—	—	—
5	106·82	15·8622	11·713	1·35414	0·9915	(0)	(0)	(0)	—
10	106·0	16·1780	11·9413	1·3547	1·0108	—	—	—	—
20	107·014	16·0964	11·9850	1·34300	1·0145	—	—	—	—
25	106·6	15·7922	11·891	1·32000	1·0066	—	—	—	—
30	107·0	15·7922	11·8823	1·33550	1·0058	5·1	1·5	6·6	4·7
50	105·4	15·3398	11·71	1·30990	0·9913	—	—	—	—
100	105·00	15·044	11·566	1·30000	0·9790	8·0	2·4	10·4	7·3
200	106·00	15·1004	11·9125	1·2676	1·0084	11·5	4·5	15·0	10·4
300	106·14	14·6800	11·6970	1·2547	0·9902	17·0	5·0	22·0	19·2
400	107·44	14·6600	11·701	1·253	0·9905	—	—	—	—
500	108·98	14·1400	11·5440	1·2248	0·9771	26·0	8·0	34·0	28·2

(*b*) Asymmetrical case (upper surface roughened)

x (mm)	δ (mm)	δ^* (mm)	θ (mm)	H	θ/θ_0	δ_1	δ_2	δ_3	δ_4
−14 (top)	73·94	15·37954	10·02147	1·53466	—	—	—	—	—
0	127·40	23·49800	15·74800	1·49210	1	—	—	—	—
25	126·04	23·21300	16·0823	1·44330	1·0212	16·0	2·5	2·5	7·5
50	126·68	22·91640	16·1863	1·41500	1·0278	—	—	—	—
100	127·48	21·82910	15·7840	1·38299	1·0022	30·0	4·0	4·0	18·0
200	127·24	20·8303	15·6329	1·33240	0·9926	—	—	—	—
400	130·33	17·87000	15·3890	1·29110	0·9772	47·0	21·0	17·0	37·0

TABLE 1. Bulk-flow parameters; all dimensions in mm. Skin friction coefficients: smooth surface 0·0024; rough surface 0·0052. For definition of 'intermittency thicknesses' δ_1 to δ_4 see figure 1; δ_τ is half-width of shear-stress perturbation profile.

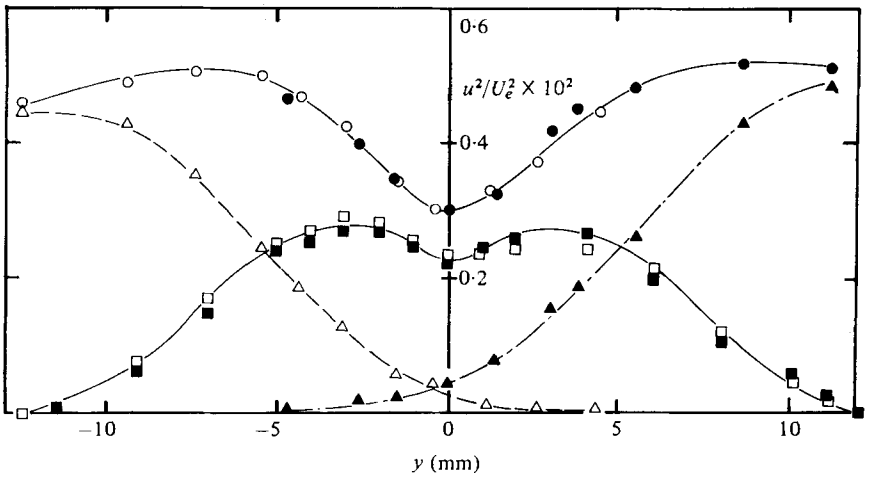

FIGURE 6. Longitudinal-component intensity profiles in symmetrical wake, $x = 100$ mm ($\simeq 2\delta_0$). ○, conventional averages; □, mixed-fluid contribution. (○, □, upper boundary layer heated; ●, ■, lower boundary layer heated.) ▲, unmixed upper-surface fluid contribution; △, unmixed lower-surface fluid contribution. Note that zone *contributions* sum to give conventional average.

that the temperature intermittency does not result solely from large-eddy time sharing (in which case the intermittency on the centre-line would be 0·5). It is of course common experience that turbulence does not mix two fluids down to molecular scales, and a recent demonstration is that by Breidenthal (1978) who used an elegant chemical technique in a two-stream mixing layer. The present results demonstrate mixing only down to scales of the order of the hot-wire length, 1 mm, but smoke-flow visualization in wake flow by P. Pongprudhanon (unpublished work at Imperial College) appeared to show mixing down to the scale of the smallest eddies (the molecular diffusion of smoke being negligible). Note that this question is different from the question of the size of the *energy-containing* eddies in the inner wake, discussed below.

Figure 5 shows that the intermittency profiles at different stations are geometrically similar and fairly close to an error-function form. The thickness δ_i given in table 1 is chosen so as to optimize the collapse and provide a convenient measure of the half-thickness of the inner wake.

Figure 6 shows the u-component intensity about two boundary-layer thicknesses downstream of the trailing edge. This station has been chosen as typical of the results for the symmetrical case; the thesis of Andreopoulos (1978) gives measurements for $x = 25$, 50, 100, 200 and 400 mm. At $x = 25$ mm, excursions caused by the sublayer, and possibly by the finite thickness of the trailing edge, are apparent, while for distances much more than 100 mm downstream a slow departure from self-preservation sets in because the inner wake extends outside the inner layers of the original boundary layers. The variation of structural parameters with x is very much smaller than the variation of the intensities. It can be seen that the contributions of upper-surface fluid, lower-surface fluid and mixed fluid to $\overline{u^2}$ are roughly proportional to their contributions to the intermittency. This implies that $\overline{u^2}$ is roughly homogeneous throughout the fluid, but this is far from true for some of the more complicated turbulence quantities described below.

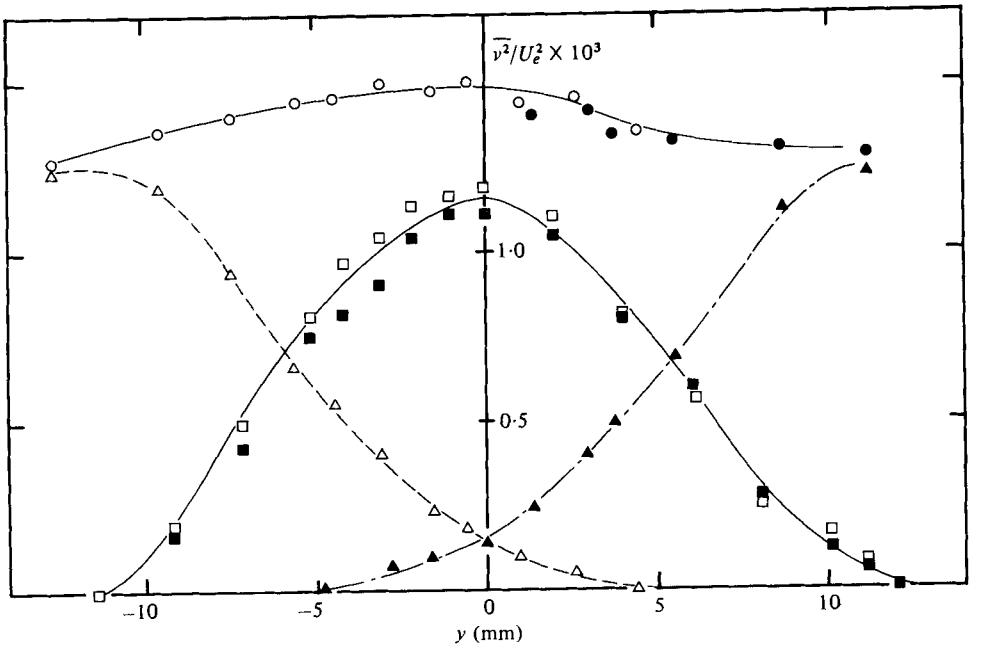

FIGURE 7. Vertical-component intensity profiles in symmetrical wake, $x = 100$ mm. Symbols as in figure 6.

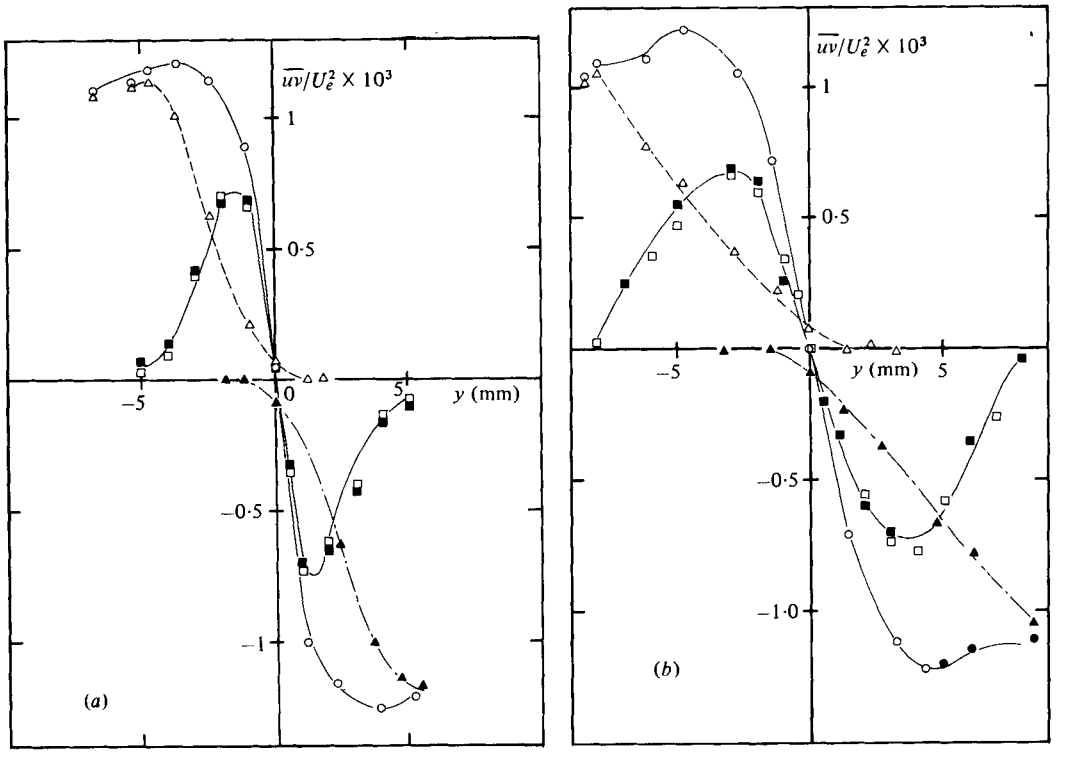

FIGURE 8(*a*, *b*). For legend see facing page.

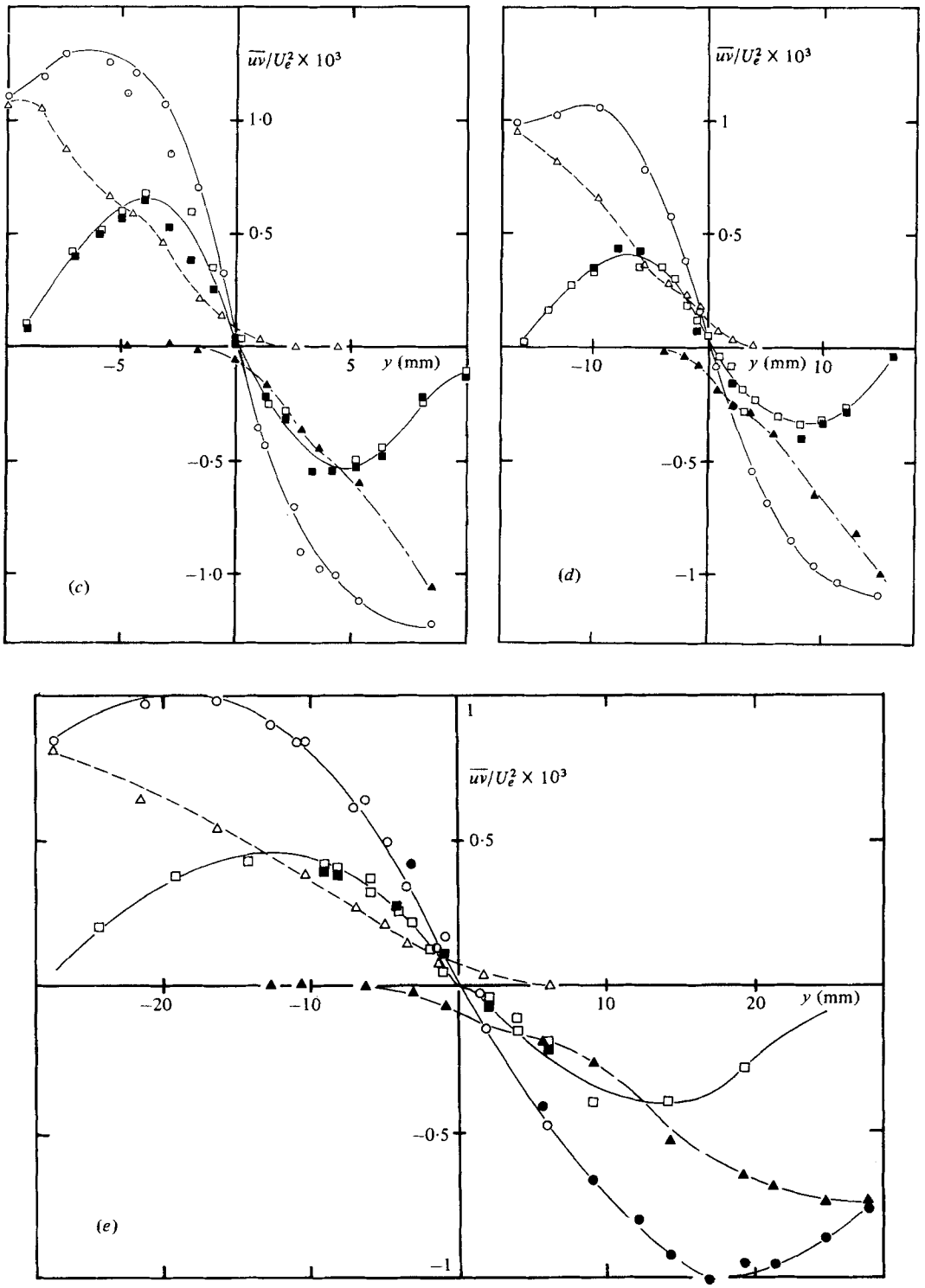

FIGURE 8. Shear-stress profiles in symmetrical wake. Symbols as in figure 6; dotted lines at top or bottom show trailing-edge profiles. (*a*) x = 25 mm; (*b*) x = 50 mm; (*c*) x = 100 mm; (*d*) x = 200 mm; (*e*) x = 400 mm.

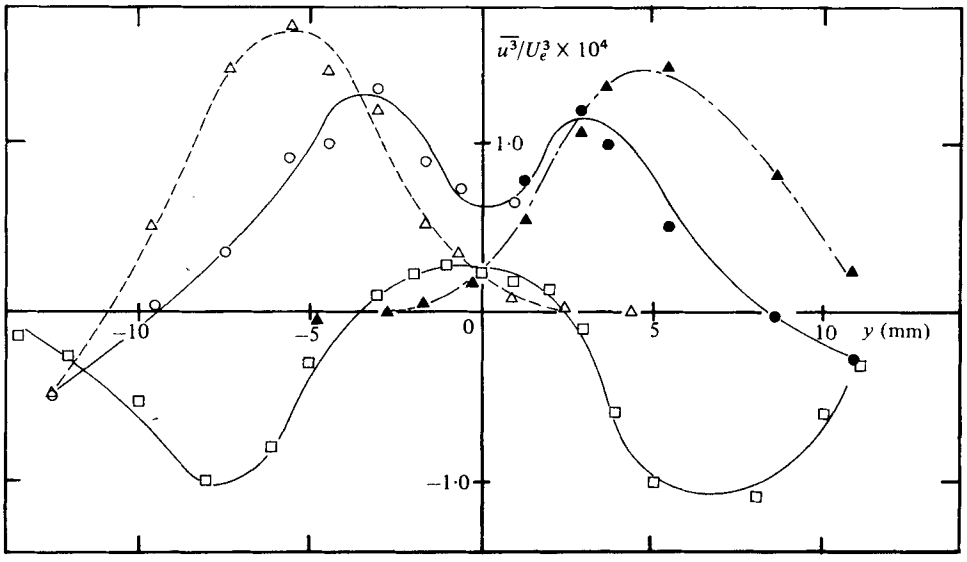

FIGURE 9. Triple-product $\overline{u^3}$ profiles in symmetrical wake, $x = 100$ mm. Symbols as in figure 6.

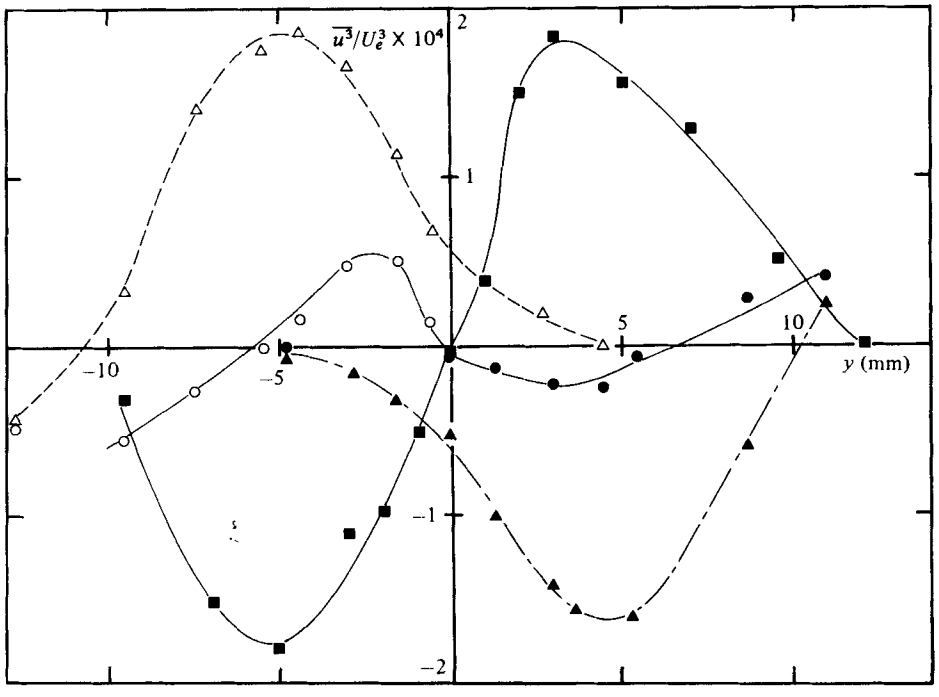

FIGURE 10. Triple-product $\overline{v^3}$ profiles in symmetrical wake, $x = 100$ mm. Symbols as in figure 6.

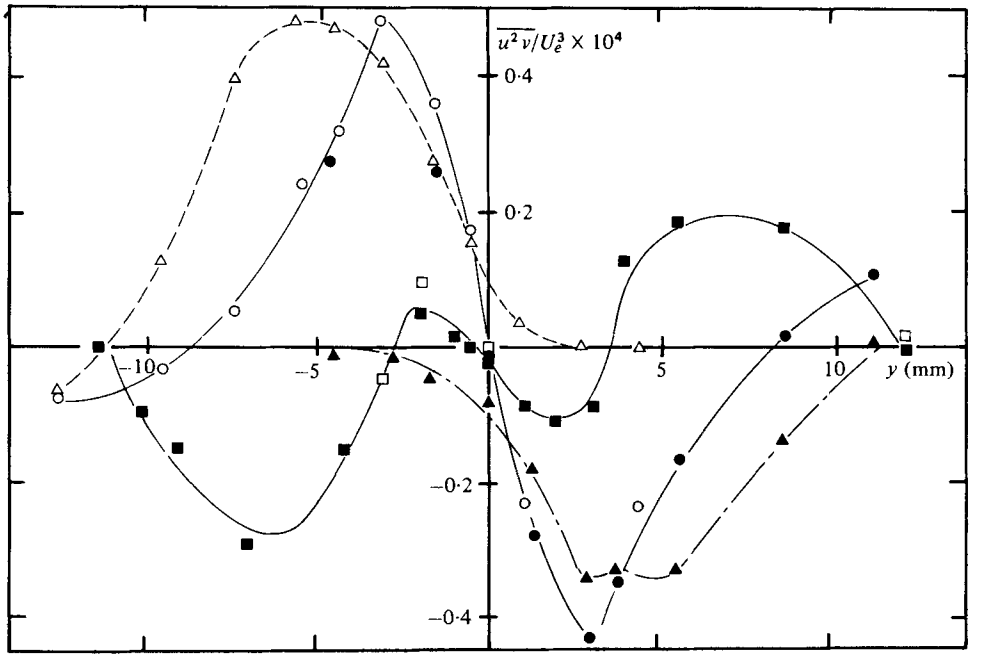

FIGURE 11. Triple-product $\overline{u^2v}$ profiles in symmetrical wake, $x = 100$ mm. Symbols as in figure 6.

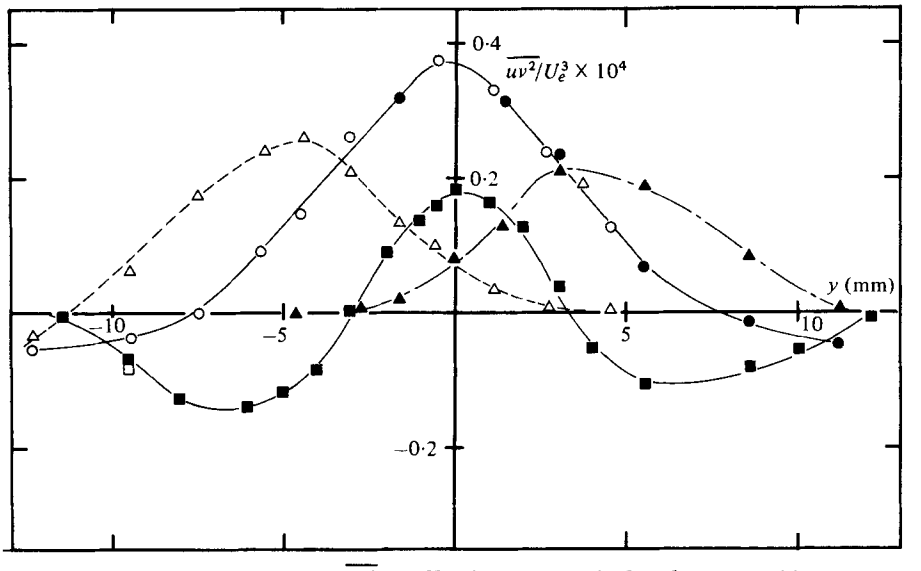

FIGURE 12. Triple-product $\overline{uv^2}$ profiles in symmetrical wake, $x = 100$ mm. Symbols as in figure 6.

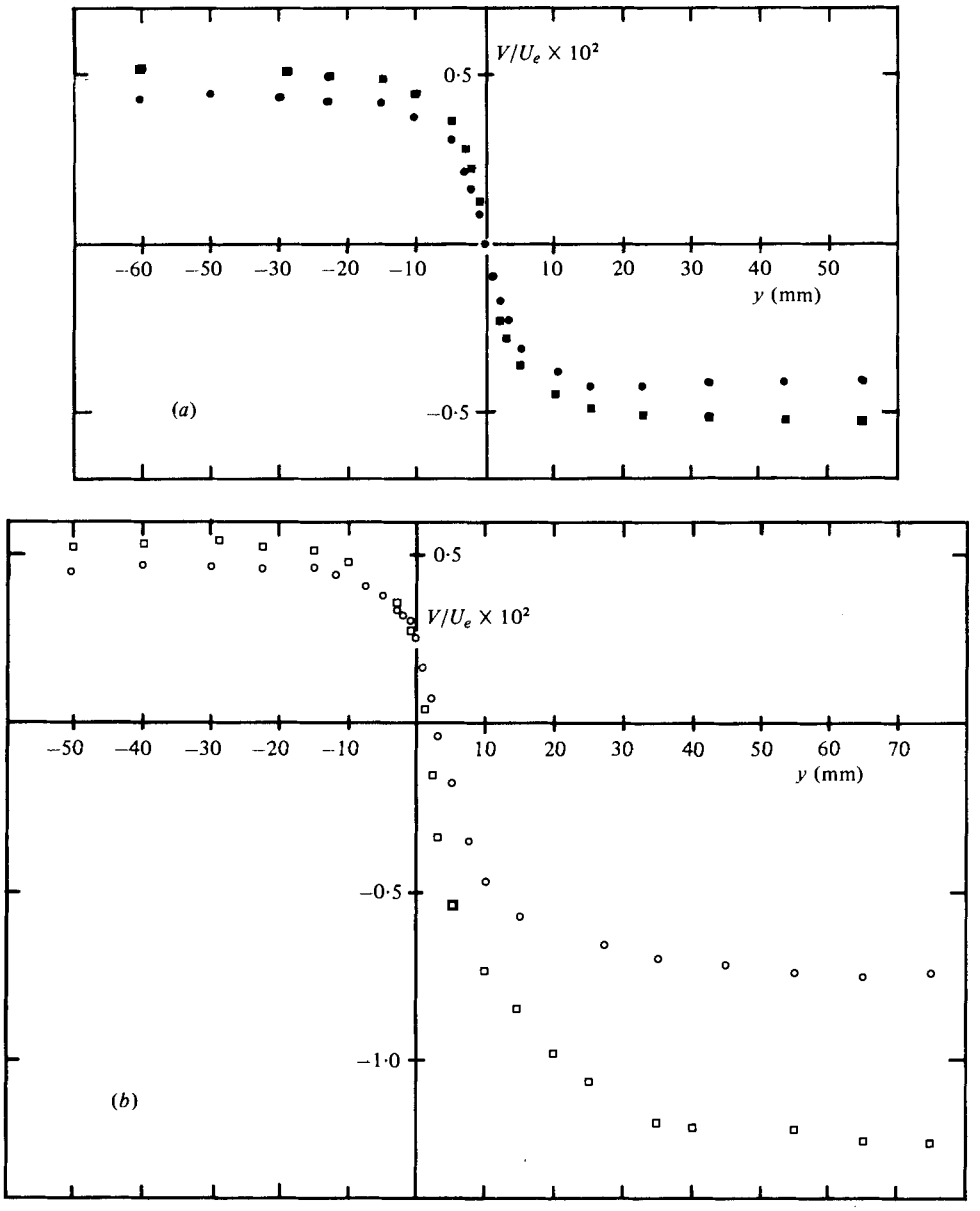

FIGURE 13. V-component mean-velocity profiles. Values of x (mm): ○, 50; □, 100. (*a*) Symmetrical wake; (*b*) asymmetrical wake.

Figure 7 shows $\overline{v^2}$, also at $x = 100$ mm, and figure 8 shows the shear-stress profiles at various distances downstream. The shear-stress profile at the trailing edge is shown dotted, and the way in which the inner wake profiles gradually move out beyond the edge of the constant-stress layer at the larger distances downstream is clearly shown. When this happens, inner-layer scaling breaks down, the profiles start to depend on the boundary-layer thickness δ and other outer-layer parameters, and eventually the structural parameters will change from values typical of a boundary layer or near wake to values typical of the self-preserving far wake.

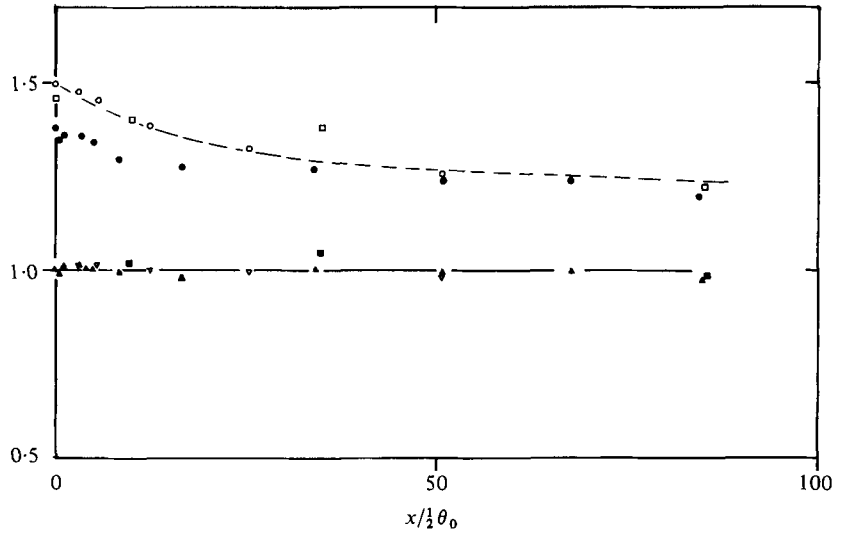

FIGURE 14. Streamwise development of integral parameters. ○, δ^*/θ_0; ▽, θ/θ_0. (○, ▽, asymmetrical wake; ●, ▼, symmetrical wake.) Results of Chevray & Kovasznay (1969): □, δ^*/θ_0; ■, θ/θ_0.

Figures 9–12 show the triple velocity products; here, large differences, including differences in sign between the contributions of different zones to the conventional average quantities, can be discerned. Briefly, the mixed-zone averages are those expected of an isolated wake, implying a general outward spread of turbulent energy and shear stress, while the unmixed-fluid averages correspond to a flow of turbulent energy *towards* the centre-line to make up for the reduction in production rate there as the mean velocity gradient changes from $O(\tau_w/\mu)$ to zero. Outside the inner wake the mixed-fluid triple products tend to the rather smaller values typical of the undisturbed boundary layer, representing outward transport of turbulent energy and shear stress.

Figure 13 shows the V-component velocity profiles in the wake for the symmetrical and asymmetrical cases. These are obtained by integration of the continuity equation, assuming $V = 0$ on the centre-line in the symmetric case; in the asymmetric case the boundary condition on V is applied at $y = \delta$, assuming that the entrainment velocity remains unchanged with x so that the V component velocity is equal to $U_e\, d\delta/dx$ minus the entrainment velocity as deduced from the boundary-layer results. This argument was applied at the edge of the upper boundary layer and satisfactorily checked at the edge of the lower boundary layer. A rough estimate of the trajectory of the trailing-edge streamline in the asymmetrical case indicates that it reaches a height of $y = 0{\cdot}3$ mm at $x = 400$ mm and its displacement is therefore negligible compared to the thickness of the inner wake. However, the slope of the trailing edge streamline is not negligible compared to the inclination of the displacement surface and would therefore have to be taken into account in a calculation. This implies that, even in the absence of any externally imposed pressure gradient, normal pressure gradients within the wake have a significant effect in producing curvature of the displacement surface.

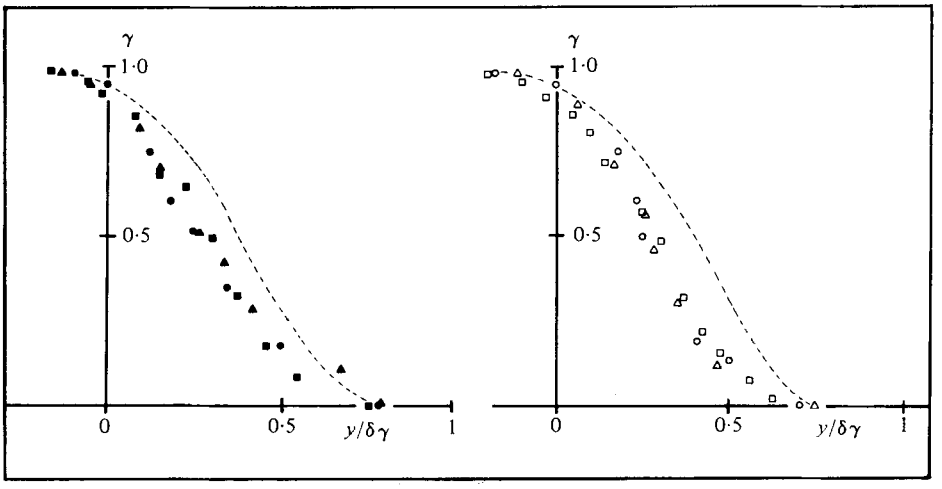

FIGURE 15. Temperature-intermittency profiles scaled by profile width δ_γ: asymmetrical wake (see table 1). Values of x (mm): ○, 25; △, 100; □, 400. (○, △, □, upper boundary layer heated; ●, ▲, ■, lower boundary layer heated). – – – –; symmetrical wake.

Figure 14 shows the variation of displacement thickness and momentum thickness, normalized by the momentum thickness at the trailing edge, for the symmetric and asymmetric cases: it also shows the results of Chevray & Kovasznay for the symmetrical case. The higher initial value of δ^*/θ in Chevray and Kovasznay's experiments is explicable by the lower Reynolds number, but the subsequent decrease seems to be very much slower than in the present case.

Figure 15 shows the intermittency (recall that the intermittency factor is the fraction of time for which the fluid is either fully 'hot' or 'warm', i.e. mixed). As expected, the curves for the case of upper (rough) boundary-layer heating and lower (smooth) boundary-layer heating are not symmetrical.

In the asymmetrical case, the intermittency profiles at different downstream distances collapse quite well together, but the profile is very much less full than the approximation to an error function observed in the symmetrical case and shown dotted in figure 15. Table 1 presents various lengths deduced from the intermittency profiles for the symmetrical and asymmetrical cases. These are defined by the highly idealized sketch in figure 1 and represent the innermost and outermost limits of the position of the interface between mixed and unmixed fluid. Here, $\delta_1 + \delta_4$ is the overall width of the inner wake while δ_2 and δ_3 represent the maximum excursions of foreign fluid over the centre-line. When the upper boundary layer is heated the thickness of the intermittency profile (the region over which the probability of finding cold fluid, $1-\gamma$, goes from 1 to 0) is $\delta_{iu} \equiv \delta_2 + \delta_4$; in $\delta_2 < y < \delta_1$, the fluid is at least 'warm' (mixed) if not 'hot' so $\gamma = 1$. When the lower boundary layer is heated $\delta_{iu} = \delta_1 + \delta_3$. In the symmetrical case, $\delta_1 = \delta_4$, $\delta_2 = \delta_3$.

4. Discussion

The experimental techniques used in the present work make plain the essential physical processes involved in shear-layer interaction, which are normally obscured in conventional averaging by the symmetry of the flow. The initial discussion can therefore be based with adequate generality on the results of the symmetrical case, and the asymmetrical case considered later as additional evidence.

4.1. *Symmetrical case*

The boundary of the inner wake of mixed fluid is most clearly identified from the intermittency profiles shown in figure 4, whose boundaries are sketched, not to scale, in figure 1 and tabulated as δ_γ in table 1. Here δ_γ is the distance between the points where $\gamma = 1$ and $\gamma = 0$; the distance from the *centre-line* to the point at which the intermittency factor decreases to 0·005, δ_1, is a more useful measure of wake half-width. A half-thickness δ_τ can be defined similarly as the distance from the centre-line to the point at which the perturbation in shear stress becomes negligible. It is somewhat less easy to estimate than δ_1: it seems to be slightly smaller initially but then grows a little more rapidly. The fact that δ_τ is nearly the same as δ_1 implies that perturbation in shear stress are confined within the average boundaries of the region of mixed fluid. This implies the interesting fact that the disappearance of the solid surface at the trailing edge, and the presumably large changes in inner-layer behaviour occasioned by the relaxation of the no-slip condition at the solid surface, have little effect on the pressure-strain redistribution term in the shear-stress transport equation outside the mixed region. (This is the main term containing the pressure fluctuations and is therefore the most likely vehicle for any 'action at a distance'.)

Measurements by Castro & Bradshaw (1976), Chandrsuda (1975) and Wood (1980) in mixing layers approaching solid surfaces show that the triple products, at least those including v, tend to be reduced by the presence of the solid surface even before the turbulent region reaches it. The present results do not, however, show any significant tendency for the triple products to *increase* downstream of the trailing edge as the constraint of the solid surface is removed. There are, of course, large changes in triple products within the region spanned by the mixed fluid.

The conventional averages of $\overline{u^2}$, $\overline{v^2}$ and $\overline{uv}$ in the wake are qualitatively the same as found in the self-preserving wake far downstream of an obstacle; that is, $\overline{u^2}$ has a minimum on the centre-line, attributable to the fact that turbulent energy production is slightly negative there ($-\overline{uv}\,\partial U/\partial y = 0$, $-(\overline{u^2}-\overline{v^2})\,\partial U/\partial x < 0$), and $\overline{v^2}$ has a barely perceptible minimum (actually not visible at all at $x = 100$ mm), while $\overline{uv}$ changes from a positive value, of the order of the wall shear stress, on one side of the inner wake to a negative value of the order of the wall shear stress on the other side. The respective contributions of the upper surface, lower surface and mixed fluid to the intensities $\overline{u^2}$ and $\overline{v^2}$ are, as already remarked, roughly the same as if all three zone averages were equal. However, this is by no means the case with $\overline{uv}$, where unmixed fluid preserves its sign of shear stress even after crossing the centre-line, while the contribution of the mixed fluid to the shear stress is antisymmetrical within the accuracy of the experiments, as expected. This behaviour of the shear stress, which is qualitatively paralleled by that of the other quantities which change sign from one side of the wake to the other, is consistent with the behaviour of the intermittency

and with the model of the flow sketched in figure 1; the instantaneous boundaries of the inner wake are highly sinuous, allowing unmixed fluid to cross the centre-line without losing the sign of its shear stress, while the mixed fluid itself behaves somewhat like an isolated wake (in what is admittedly a highly turbulent 'free stream').

The triple-product $\overline{u^3}$ (figure 9) shows the first really spectacular difference between zonal averages. The conventional average value of $\overline{u^3}$ reaches about $1 \times 10^{-4} U_e^3$ at the trailing edge, near the centre-line. The conventional average on the centre-line in the wake falls, following the behaviour of $\overline{u^2}$, while the conventional-average values at the outer edges of the inner wake are, if anything, slightly higher than in the boundary layer. This behaviour of the conventional average, however, completely disguises the fact that a mixed-fluid contribution of opposite sign appears. As in the case of the mixed-fluid contribution to $\overline{uv}$, the distribution of mixed-fluid $\overline{u^3}$ is rather like that which would be found in an isolated wake, with negative values near the edges and positive values near the centre-line. The unmixed fluid near the edges of the inner wake acquires positive values of $\overline{u^3}$ larger than any found in the boundary layer at the trailing edge. Positive values of $\overline{u^3}$ imply the presence of positive-going spikes in the u signal; the converse also holds. We conclude that the mixed-fluid excursions around the mean U-component velocity near the edge of the inner wake, where $\overline{u^3}$ is negative, consist of occasional negative-going spikes; these are presumably caused by eruptions of fluid from nearer the centre-line, where the mean u-component velocity is smaller, separated by rather longer intervals in which the instantaneous U-component velocity within the warm fluid is rather greater than the mean. (It must be remembered in this discussion that the velocity traces within the different zones are not necessarily continuously defined, the u-component fluctuation within the mixed zone, for instance, being defined *only* within the mixed zone; this prevents the quantitative analysis of time-domain information by normal methods, but does not invalidate the present discussion.) The u-component velocity fluctuation within the unmixed fluid at the outer edge of the inner wake evidently consists of occasional positive-going spikes, presumably associated with the inrush of faster-moving fluid from further out in the flow, interspersed with longer regions of small negative u. In terms of the 'burst' and 'sweep' model of the inner layer of the attached turbulent boundary layer, the in-going sweeps are naturally associated with unmixed fluid from further out in the flow, while the bursts transport mixed fluid from nearer the centre-line. A quantitative comparison of the present results with boundary-layer data would require measurements in a boundary layer whose surface was heated only downstream of a given line, as in the experiment of Johnson (1959). We hope to make conditional sampling measurements in such a flow at a later date. At the moment, however, one may conclude that the burst-and-sweep cycle in the boundary layer is not destroyed when the flow passes over the trailing edge, but there must be inevitable quantitative differences because the eddy size is no longer constrained to a nominal value of zero on the centre-line.

The product $\overline{u^3}$ does not appear in any of the major terms in transport equations for Reynolds stress, but the derivatives of $\overline{v^3}$ and $\overline{u^2 v}$ in the y direction appear in the turbulent transport ('diffusion') term in the turbulent energy equation. These quantities are shown in figures 10 and 11. The conventional-average values of $\overline{v^3}$ at $x = 100$ mm appear not to be accurately antisymmetrical as required; values at other stations are more reasonable and the part of the curve for y greater than zero in

figure 10 should be ignored. Conventional-average values of $\overline{u^2v}$, shown in figure 12, are acceptably antisymmetrical in the main part of the boundary layer. The products $\overline{v^3}$ and $\overline{u^2v}$ generally have the same sign as y, but both have a small region of changed sign close to the surface in the boundary layer at the trailing edge and this continues, slightly augmented, in the conventional averages in the wake. The mixed- and unmixed-fluid contributions differ from the conventional averages even more spectacularly than in the case of $\overline{u^3}$. The mixed-fluid contribution comprises a transport of turbulent energy away from the centre-line while the unmixed-fluid contribution implies a transport of turbulent energy towards the centre-line. It should be noted that quantitative energy balances for the separate zones cannot be deduced without measurements of the average value of the energy transfer across the instantaneous boundary between the zones; we have not yet attempted the rather delicate measurements of point-conditioned statistics that would be required. There is, of course, a continuous advection of turbulent energy by the mean velocity across the *mean* boundary between the mixed- and unmixed-fluid zones because this boundary is not a streamline. It is noteworthy that values of $\overline{v^3}$ found in the inner wake are somewhat larger than those found in the main part of the boundary layer; for instance, $\overline{v^3}$ at $x = 0$ attains a maximum value of only about $1 \times 10^{-5} U_e^2$ at $y \simeq 0{\cdot}5\delta$ while the mixed-fluid contribution to $\overline{v^3}$ reaches about twice this value at $y \simeq 0{\cdot}5\delta_i$. The rate of growth of the half-width of the inner wake, δ_i, is about 0·1 (actually varying as $x^{0{\cdot}7}$ approximately as remarked above), which is very much larger than the rate of growth of an isolated boundary layer and can be attributed to the large values of $\overline{u^2v}$ and $\overline{v^3}$ in the mixed fluid. However, a quantitative discussion is better phrased in terms of the turbulent transport velocities defined below.

The mixed-fluid contribution to $\overline{u^3}$ on the centre-line is fairly small because $\overline{u^3}$ itself has a minimum on the centre-line, and the centre-line values of mixed-zone contributions to $\overline{u^2v}$ and $\overline{v^3}$ are zero by symmetry; however the centre-line value of $\overline{uv^2}$ shown in figure 12 is numerically rather larger than the values obtained in the mixed fluid near the edges of the inner wake. The conventional average $\overline{uv^2}$ is, of course, symmetrical about the centre-line; in the boundary layer at the trailing edge it is negative everywhere, except very close to the surface, where a maximum value of about $5 \times 10^{-6} U_e^3$ is obtained, compared to a maximum negative value of about $1{\cdot}5 \times 10^{-5}$ at $y \simeq 0{\cdot}5\delta$. The negative values in the mixed-fluid contribution near the edges of the inner wake are also about $1{\cdot}5 \times 10^{-5} U_e^3$, while the positive value on the centre-line is about twice this. The unmixed-fluid contribution is positive everywhere, except at the extreme edges of the inner wake where it rejoins the slightly negative conventional-average value. The measurements of $\overline{uv^2}$ are compatible with the other triple products, and imply that shear stress is transported towards the centre-line by the unmixed fluid, while the mixed fluid transports shear stress away from the centre-line in the outer parts of the inner wake but towards the centre-line in the inner part of the inner wake ($|y|$ less than 3 mm, say, in figure 12). This sense of shear-stress transport within the mixed fluid is consistent with the sign of mixed-fluid shear-stress gradient shown in figure 8; the same is broadly true of the unmixed-fluid contribution and indeed of the conventional average itself.

In all respects, therefore, the results are qualitatively compatible with the postulated model of an inner wake consisting of 'hot' and 'cold' fluid from opposite sides of the plate so finely mixed that (at least with the frequency and spatial resolution

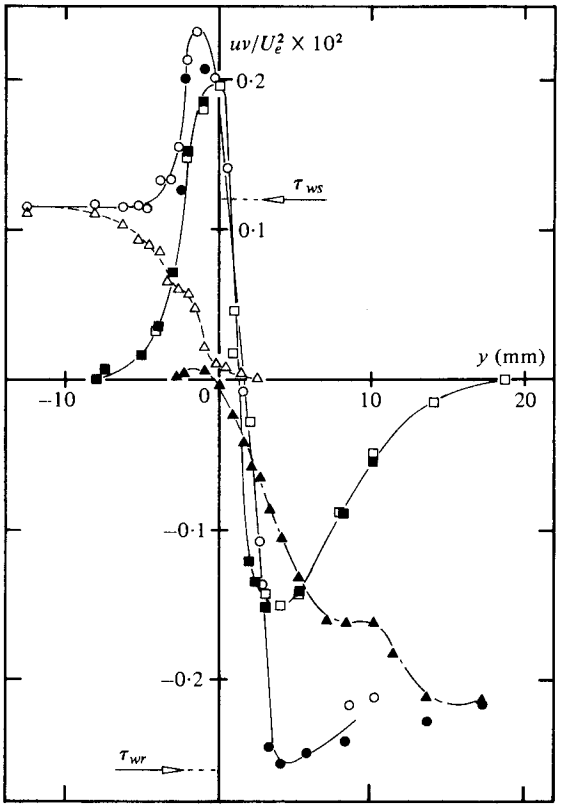

FIGURE 16. Shear-stress profiles in asymmetrical wake, x = 25 mm. Symbols as in figure 6.

available with the present instrumentation) the fluid temperature never falls to the 'cold' value. Turbulent energy transport within this inner wake is always from the centre-line, although shear-stress transport is towards the centre-line in the innermost part of the inner wake, as might be expected because the shear stress falls to zero at the centre-line. Considerable structural changes occur in the unmixed fluid in the region near the mean edges of the mixed fluid region. However, these changes seem to be confined approximately to the time-sharing or intermittent region, i.e. to positions nearer the centre-line than the outermost excursions of mixed fluid. This is partly a coincidence and does not necessarily imply that changes to the structure of the turbulence in the unmixed fluid are rigorously confined to a region between the 'peaks' and 'troughs' of the mixed/unmixed interface excursion shown in figure 1, but for practical purposes only the fully mixed region and the time-sharing region need be given special consideration in a calculation method.

4.2. *Asymmetrical case*

The skin friction coefficients on the rough and smooth sides were 0·0052 and 0·0024 respectively. The profiles of mean velocity, Reynolds stresses and triple products, given by Andreopoulos (1978), are accordingly asymmetrical (or not perfectly anti-symmetrical) but present few features that could not be deduced qualitatively from

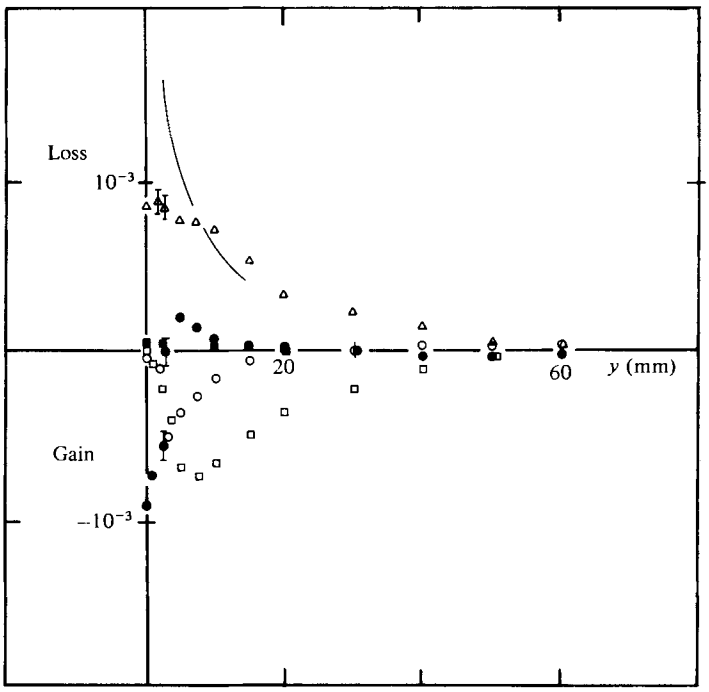

FIGURE 17. Turbulent energy balance in symmetrical wake, $x = 100$ mm. □, shear production $\overline{uv}\,\partial U/\partial y$; ■, normal-stress production $(\overline{u^2}-\overline{v^2})\,\partial U/\partial x$; ○, advection (assuming $\overline{w^2} = 0{\cdot}5(\overline{u^2}+\overline{v^2})$); ●, diffusion (assuming $\overline{pv} = 0$, $\overline{vu^2} = 0{\cdot}5(\overline{u^2v}+\overline{v^3})$); △, dissipation (by difference).

the symmetrical results. One new feature, shown in figure 16, is the appearance of a peak in conventional-average shear stress on the smooth side, $y < 0$, downstream of the trailing edge. (At the trailing edge the shear-stress profiles approach monotonically to the surface shear-stress values shown by the arrows.) The conditional averages show that the main contribution to the peak comes from the mixed fluid, whose contribution to $\overline{uv}$ is not too far from antisymmetrical. Evidently the peak results from the excursion of high-intensity rough-surface fluid, incidentally mixing with smooth-surface fluid, into a region of high mean-velocity gradient, thus leading to a large zonal value of $\overline{v^2}\,\partial U/\partial y$ (the generation term in the shear-stress transport equation). The peak is still noticeable at $x = 100$ mm but has died out by $x = 400$ mm. A few further illustrative results for the asymmetrical case are presented below.

4.3. *Transport equations*

Figure 17 shows the turbulent kinetic energy balance for the symmetrical wake at $x = 100$ mm, corresponding to the profiles presented above. Dissipation was measured by difference, neglecting the contribution of the pressure–velocity correlation $\overline{p'v}$ to the diffusion term. It is noticeable that the triple-product diffusion term changes sign, and changes quite rapidly, near the centre-line, while the dissipation by difference behaves smoothly. If the pressure–velocity term were significant and if it varied in the same way as the triple product, the dissipation by difference would also vary rapidly near the centre-line; the fact that it does not do so gives one *some* confidence that pressure–velocity correlations are not important and that the dissipation by

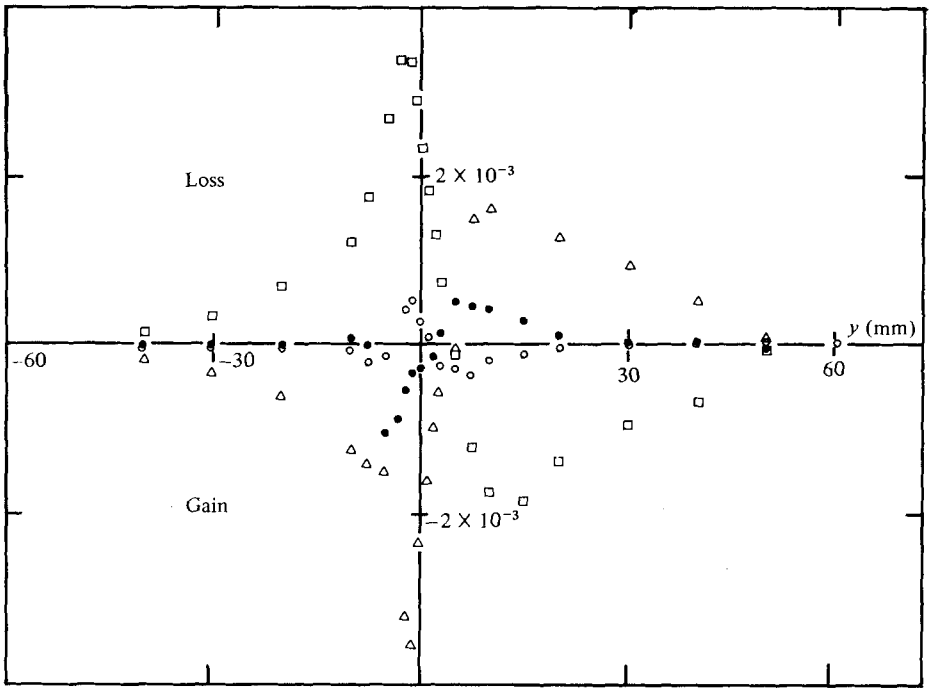

FIGURE 18. Shear-stress balance in asymmetrical wake, $x = 100$ mm. □, generation $\overline{v^2}\partial U/\partial y$; ○, mean transport; ●, turbulent transport; △, pressure–strain 'redistribution' (by difference).

difference adequately represents the true dissipation. Because $\partial U/\partial x$ is quite large, production of turbulent energy by normal stresses is significant, although still very much smaller than production by the main shear-stress term except close to the centre-line. The solid line is the inner-layer level of dissipation, which crosses the actual dissipation curve at about $y/\delta = 0{\cdot}2$, the edge of the inner layer, as expected. The gain by advection (that is, the decrease of turbulent kinetic energy along a streamline) rises to a value almost equal to the maximum production rate, and the maximum value of diffusion indeed exceeds the maximum production. Clearly the inner wake is very far from being a local-equilibrium flow, and attempts to treat it by local-equilibrium concepts like mixing length or eddy viscosity are unlikely to succeed. The energy balance in the asymmetrical case is generally similar except for a large peak in shear-stress production, corresponding to the peak in shear stress shown in figure 16 which is accompanied by a large peak in $\partial U/\partial y$. The production peak is balanced mainly by diffusion; the dissipation varies smoothly.

Figure 18 shows the terms in the shear-stress transport equations in the *asymmetrical* case. Again, a peak appears in the main generation term and is balanced by a peak in the pressure/rate-of-strain 'redistribution' term (obtained by difference). Unfortunately, of course, it is not possible to separate the redistribution term into its two constituents, which depend respectively on the mean-strain rate and on the turbulent fluctuations alone. The former constituent should strictly be grouped with the generation (to which it would make a negative contribution) and, while this group and the residual part of the pressure–strain term would certainly be larger than the transport terms, they would not exceed them by such a large factor as appears in figure 18.

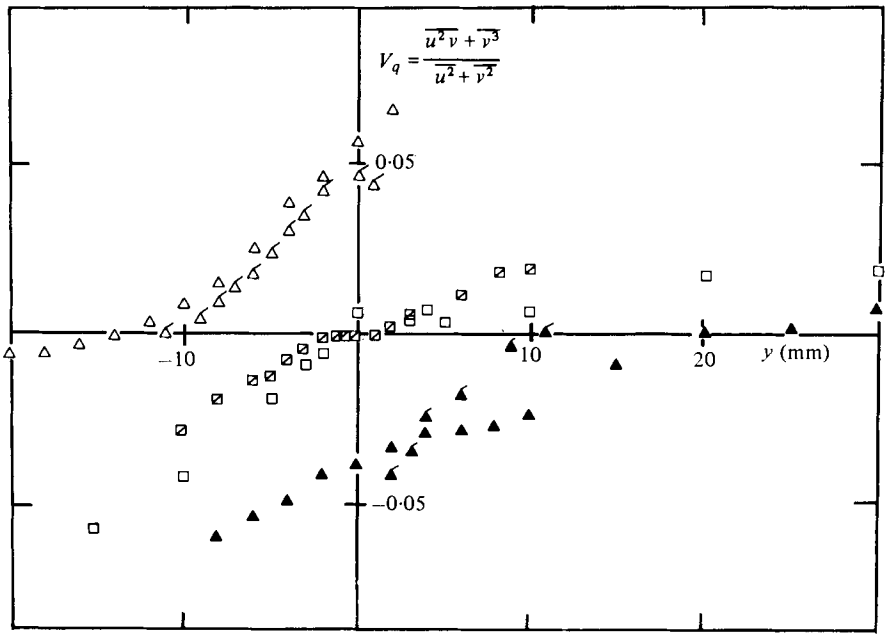

FIGURE 19. Transport velocity for turbulent energy, $V_q = (\overline{u^2v} + \overline{v^3} + \overline{vw^2})/(\overline{u^2} + \overline{v^2} + \overline{w^2})$ in mixed and unmixed fluid, assuming $\overline{w^2} = 0{\cdot}5(\overline{u^2} + \overline{v^2})$ and $\overline{vw^2} = 0{\cdot}5(\overline{u^2v} + \overline{v^3})$. Symbols as in figure 6; upper surface roughened: □, △, ▲, asymmetrical wake; ▨, ◬, ◭, symmetrical wake.

Indeed, if the shear-stress balance could be so partitioned, it would probably resemble the turbulent energy balance rather closely, except near points of zero shear stress. Since the values of generation are reasonably reliable and the transport terms are small, the sharp peak in the pressure–strain term is presumably real and implies that terms containing pressure can have quite large spatial gradients even in the absence of the solid surface. One may, however, speculate that the sharp peak is attributable mainly to the mean-strain-dependent part of the pressure fluctuation; since it occurs this is at least some indication that that term can be acceptably related to a local value of mean-velocity gradient, rather than depending significantly on a weighted average of the mean rate of strain over a large volume.

One of the key processes in the interaction of the different zones is the transport of turbulent energy or of shear stress by the turbulence itself. Gradient diffusion and the evaluation of gradients from measured values both being dubious processes, it is simplest to discuss the results in terms of the turbulent transport defined as

$$V_q = \left(\frac{\overline{p'v}}{\rho} + \tfrac{1}{2}\overline{q^2v}\right) \Big/ \tfrac{1}{2}\overline{q^2} \simeq (\overline{u^2v} + \overline{v^3})/(\overline{u^2} + \overline{v^2}), \tag{2}$$

$$V_\tau = \left(\frac{\overline{p'u}}{\rho} + \overline{uv^2}\right) \Big/ \overline{uv} \simeq \overline{uv^2}/\overline{uv}. \tag{3}$$

The transport velocity for turbulent kinetic energy, V_q, is plotted in figure 19 and that for shear stress in figure 20. The velocity of transport of turbulent energy towards the centre-line from the unmixed fluid on the smooth side of the asymmetrical wake is almost exactly the same as that for the symmetrical wake and the same applies to

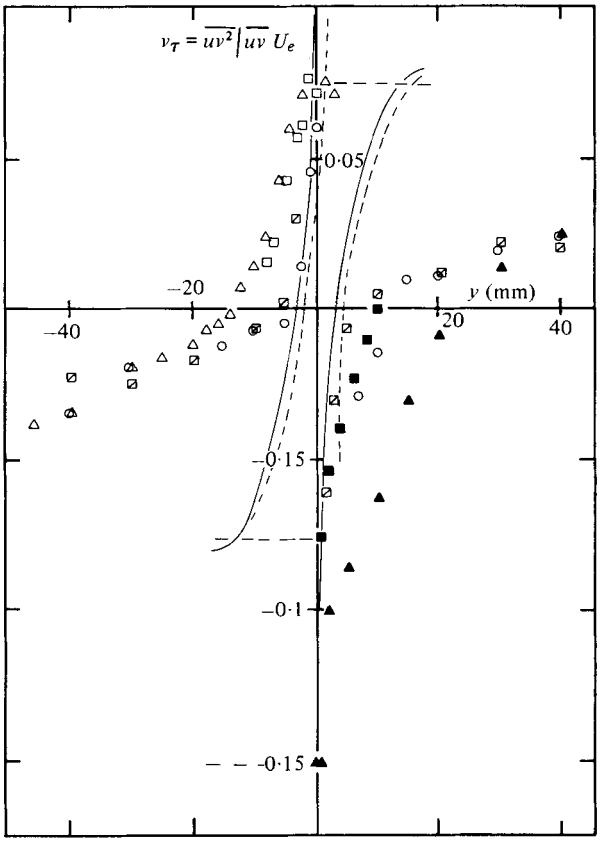

FIGURE 20. Transport velocity for shear stress, $V_T = \overline{uv^2}/\overline{uv}$; conventional averages and *unmixed* fluid averages only. Symmetrical wake: □, conventional average; ■, unmixed upper-surface fluid average; □, unmixed lower-surface fluid average. Asymmetrical wake: ○, conventional average; △, unmixed (rough) upper-surface fluid average; △, unmixed lower-surface fluid average.

the shear-stress transport velocity. There are, as expected, considerable differences between these values and the velocities of transport of unmixed-fluid energy or shear stress from the *rough* side towards the centre-line. However, the fact that the velocities of transport from the smooth side are unchanged from the symmetrical case is a strong indication that this transport depends only on the smooth wall boundary layer and not on the boundary layer on the other side. It is implied that the main reason that this transport occurs is the absence of the solid surface, that is, of the condition $v = 0$ at the centre-line, rather than the details of formation of the wake. The velocity of transport of turbulent energy from the rough-side boundary layer across the centre-line is rather smaller than the transport from the smooth side, but the opposite is true of the shear stress. Insofar as one can deduce asymptotic values for the shear-stress transport velocity at the inner edges of the unmixed fluid, they appear to be about 7 % of the free-stream velocity on the smooth side and 15 % of the free-stream velocity on the rough side. That is, the shear-stress transport velocity on either side appears to be directly proportional to the general level of shear stress on that side,

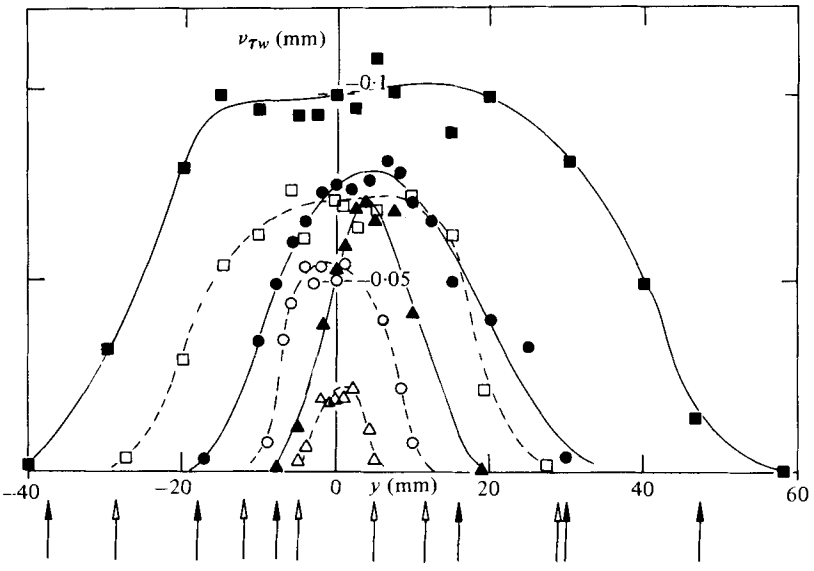

FIGURE 21. Mixed ('warm') fluid eddy viscosity $\nu_{Tw} \equiv -\overline{uv_w}/(U_e\,\partial U/\partial y)$ mm. △, x = 25 mm; ○, x = 100 mm; □, x = 400 mm. △, ○, □, symmetrical wake; ▲, ●, ■, asymmetrical wake.

rather than to the square root of shear stress as simple dimensional analysis would require. The same rather unsatisfactory feature is found in the data correlation for shear-stress transport velocity used by Bradshaw, Ferris & Atwell (1967). The transport velocity of the mixed-fluid shear stress, defined as $V_{Tm} = \overline{uv_m^2}/\overline{uv_m}$, also attains about 7 % of the free-stream velocity at the edges of the inner wake but is, of course, directed outwards at each edge.

Figure 21 shows the eddy viscosity made with the mixed-fluid shear stress and the conventional-average mean-velocity gradient. In all cases the numerator and denominator pass through zero at virtually the same point, and the eddy viscosity is a well-behaved function looking remarkably like that in an isolated wake. The profiles in the asymmetrical wake are, of course, themselves asymmetric, but, as a class, seem to scale quite satisfactorily on the local width of the mixed-fluid shear stress profile. To within the general accuracy of the measurements the maximum level of eddy viscosity appears to scale satisfactorily on the width of the inner wake also. In the symmetrical case the velocity scale required is uncontroversially u_τ but in the asymmetrical case the relevant velocity scale is some weighted mean of the friction velocities on the rough and smooth sides, and it appears that a simple average or even geometric mean may be adequate. It is at first sight highly remarkable that the mixed-fluid eddy viscosity should be such a well-behaved quantity in what is obviously a rather complicated flow. The explanation appears to be that the mixed fluid is mixed by the extremely small eddies coming from close to the surface in the original boundary layers, the eddy length scale being roughly proportional to the distance from the surface. This means that the eddy length scale well within the mixed-fluid region of the near wake is likely to be considerably smaller than in an isolated shear layer of the same thickness – that is, the energy-containing eddies will be considerably smaller than the wake width. Note again that the size of the *energy-containing* eddies is not

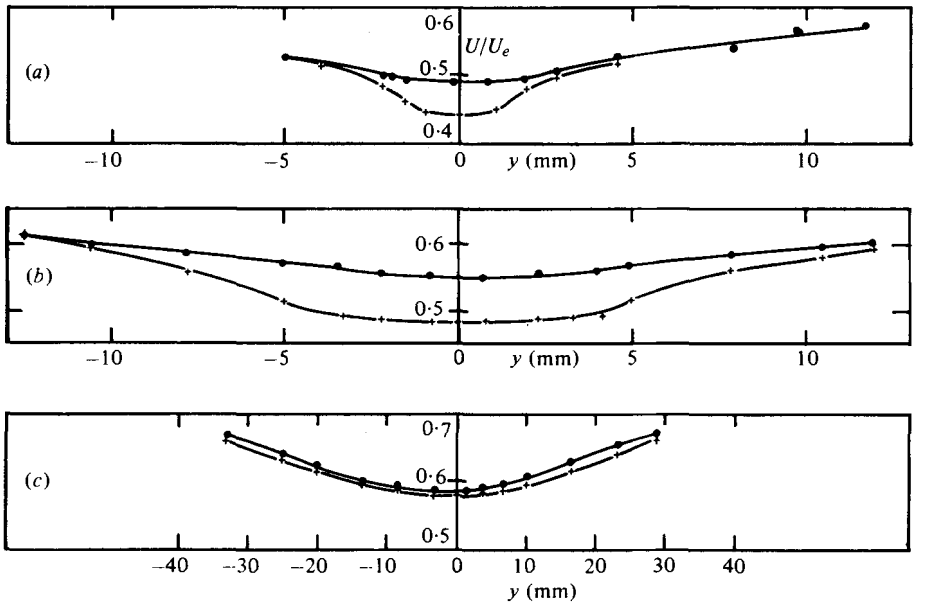

FIGURE 22. Mixed ('warm') fluid mean velocity in symmetrical wake. +, mixed-fluid average; ○, conventional average (from *hot-wire* results, for best basis of comparison). (*a*) x = 25 mm; (*b*) x = 100 mm; (*c*) x = 400 mm (reduced y scale).

directly related to fineness of mixing in the 'warm fluid', which depends on the *smallest* eddies. The smaller the ratio of eddy length scale to mean flow length scale the closer the flow is likely to approach to the ideal conditions of very small eddy length scale or 'mean free path' required for the eddy-viscosity or gradient-diffusion concepts to be theoretically valid. This explanation is at least sufficiently plausible to suggest that the mixed-fluid eddy viscosity is likely to be well behaved in all kinds of inner wakes, although that is not to say that the simple scaling which has proved adequate here will necessarily be accurate in more highly asymmetrical interactions. The mixed-fluid eddy viscosity made with the velocity gradient in the mixed fluid would differ significantly from that made with the conventional-mean velocity gradient and, from a fundamental viewpoint, the former definition might be preferable. In calculation methods, however, one would prefer to avoid carrying a separate mean-momentum equation for mixed fluid; inter-zone momentum transfer could not be neglected. Figure 22 shows that the mixed-fluid mean velocity appears to approach the conventional mean velocity at large distances downstream. The asymmetrical wake results are similar but the difference between the two velocities decreases more slowly with distance downstream.

We do not attempt in the present work to produce detailed formulae for the structural changes within the unmixed fluid or the eddy viscosity within the mixed fluid. However, our work in progress suggests that an adequate calculation method for asymmetric wakes can be founded on a three-layer model like that expounded in the present paper, the outer unmixed layers being calculated by the transport equation models with allowances for the structural changes and time sharing at the edges of the inner wake, together with a representation of the shear-stress contribution of the inner (mixed) wake itself by means of an eddy viscosity.

5. Conclusions

Detailed measurements of turbulent quantities in the symmetrical and asymmetrical wakes of thin, flat plates have provided support for a three-layer model of the flow generally as sketched in figure 1. The inner wake proper consists of finely mixed fluid, some from the upper and some from the lower boundary layer, which is expected to have a comparatively small eddy length scale; the larger undulations of the interface shown in figure 1 are likely to be imposed by the turbulence in the outer part of the flow, which is relatively unchanged from the original boundary layers. Significant changes occur in the structure of the unmixed fluid but they appear to be confined to within the intermittent region, that is, between the 'crests' and 'troughs' of the interface between the mixed and unmixed fluid.

Temperature-conditioned sampling has proved an extremely effective method of distinguishing these three regions and the accuracy of the present results appears to be good. The most spectacular differences between conventional and conditional averages occur in the triple products, that is in the terms which contribute to turbulent transport of turbulent kinetic energy and shear stress in the normal direction. Turbulent transport plays a key role in the balance of turbulent kinetic energy. The results for conditional-average dimensionless triple products and other turbulence structure parameters are believed to be sufficiently accurate to serve as a guide to calculation methods. The present authors and their colleagues have already done some work on a calculation method based on the use of shear stress transport equations for the outer regions, with allowance for structural changes and time-sharing phenomena, together with an eddy-viscosity formula to represent the shear stress in the inner mixed region.

We are grateful to Mr D. H. Wood and Dr P. H. Hoffmann for helpful discussions and to Dr A. D. Weir for assisting with the earlier experimental work. We wish to acknowledge the financial support of the Science Research Council and of the Greek State Scholarship Establishment (IKY).

REFERENCES

ANDREOPOULOS, J. 1978 Symmetric and asymmetric near wake of a flat plate. Ph.D. thesis, Imperial College, London (available on microfiche).

ANDREOPOULOS, J. & BRADSHAW, P. 1980 Measurements of turbulence structure in the boundary layer on a rough surface. *Boundary Layer. Met.* (to appear).

BRADSHAW, P. 1975 *Trans. A.S.M.E.* I, *J. Fluids Engng* **97**, 146.

BRADSHAW, P. 1976 *Theoretical and Applied Mechanics* (ed. W. T. Koiter), p. 103. North-Holland.

BRADSHAW, P., DEAN, R. B. & MCELIGOT, D. M. 1973 *Trans. A.S.M.E.* I, *J. Fluids Engng* **95**, 214.

BRADSHAW, P., FERRISS, D. H. & ATWELL, N. P. 1967 *J. Fluid Mech.* **28**, 593.

BREIDENTHAL, R. E. 1978 A chemically reacting turbulent shear layer. Ph.D. thesis, California Institute of Technology.

CASTRO, I. P. & BRADSHAW, P. 1976 *J. Fluid Mech.* **73**, 265.

CHANDRSUDA, C. 1975 A reattaching turbulent shear layer in incompressible flow. Ph.D. thesis, Imperial College, London.

CHEVRAY, R. & KOVASZNAY, L. S. G. 1969 *A.I.A.A. J.* **7**, 1641.

DEAN, R. B. & BRADSHAW, P. 1976 *J. Fluid Mech.* **78**, 641.

FABRIS, G. 1976 Conditionally sampled turbulent thermal and velocity fields in the wake of a warm cylinder and its interaction with an equal cool wake. Ph.D. thesis, Illinois Institute of Technology.

HOFFMANN, P. H. & BRADSHAW, P. 1978 Turbulent boundary layers on surfaces of mild longitudinal curvature. *Imperial College, Aero Rep.* 78–04.

HUFFMAN, G. D. & NG, B. S.-H. 1978 *A.I.A.A. J.* **16**, 193.

JOHNSON, D. S. 1959 *Trans. A.S.M.E.* E, *J. Appl. Mech.* **24**, 325.

LARUE, J. C. & LIBBY, P. A. 1978 *Phys. Fluids* **21**, 891.

MOREL, T. & TORDA, T. P. 1973 *A.I.A.A. J.* **12**, 533.

MURLIS, J., TSAI, H. M. & BRADSHAW, P. 1980 The structure of turbulent boundary layers at low Reynolds number. Submitted to *J. Fluid Mech.*

PALMER, M. D. & KEFFER, J. F. 1972 *J. Fluid Mech.* **53**, 38.

WEIR, A. D. & BRADSHAW, P. 1974 Apparatus and programs for digital analysis of fluctuating quantities in turbulent flow. *Imperial College, Aero Rep.* 74–09.

WEIR, A. D., WOOD, D. H. & BRADSHAW, P. 1980 Interaction of two parallel turbulent mixing layers in a jet. *J. Fluid Mech.* (to appear).

WOOD, D. H. 1980 A reattaching, turbulent, thin shear layer. Ph.D. thesis, Imperial College, London.